P-Glycoprotein (Abcb1) is involved in absorptive drug transport in skin

doi: 10.1016/j.jconrel.2008.08.004

P-Glycoprotein (Abcb1) is involved in absorptive drug transport in skin

Katsuaki Ito[a)], Hai Thien Nguyen[a)], Yukio Kato[a)], Tomohiko Wakayama[b)], Yoshiyuki Kubo[a)], Shoichi Iseki[b)] and Akira Tsuji[a)]*

[a)]Division of Pharmaceutical Sciences, Graduate School of Natural Science and Technology, Kanazawa University, Kakuma-machi, Kanazawa 920-1192 and [b)]Department of Histology and Embryology, Graduate School of Medical Science, Kanazawa University, Takara-machi, Kanazawa 920-8641, Japan.

*Corresponding author. Tel.: +81 76-234-4479; fax: +81 76-264-6284.

E-mail address: tsuji@kenroku.kanazawa-u.ac.jp (A. Tsuji)

Abstract

The purpose of the present study was to investigate the role of P-glycoprotein (P-gp) in drug disposition in skin. The distribution of P-gp substrates (rhodamine 123 and itraconazole) to the skin after administration from the epidermal side was lower in P-gp gene knockout (*mdr1a/1b*$^{-/-}$) mice than that in wild-type mice. Coadministration of propranolol, a P-gp inhibitor, decreased the distribution of itraconazole to the skin in wild-type mice, but not in *mdr1a/1b*$^{-/-}$ mice. These results suggest that P-gp contributes to the influx (from the epidermal side) of its substrates into skin, although P-gp is generally involved in efflux of drugs from various tissues. This finding was supported by the lower vectorial transport of rhodamine 123 from the epidermal to the hypodermal side in *mdr1a/1b*$^{-/-}$ mice in Ussing-type chamber experiments and by the immunohistochemical localization of P-gp throughout the dermal layer. Distribution of itraconazole after intravenous administration, on the other hand, was higher in *mdr1a/1b*$^{-/-}$ mice than that in wild-type mice, suggesting that P-gp transports this drug from the skin to the circulation. The present findings are the first to demonstrate involvement of P-gp in dermal drug disposition.

KEY WORDS: Skin; Transporter; P-glycoprotein; ABCB1; Transdermal permeation

Introduction

Skin acts as a barrier against environmental stress and plays pivotal roles in homeostasis, including maintenance of body temperature and water balance. Stratum corneum (SC), the outermost layer of skin, is generally considered as a major barrier against environmental stress, and penetration of xenobiotics through the epidermal layer is quite limited due to the SC structure, which includes multiple lipid lamellae [1]. In addition to such physical barriers, there is increasing evidence that skin epithelial cells contain biochemical barrier systems [2-5]. These include metabolic enzymes expressed in skin keratinocytes that convert various types of xenobiotic compounds into hydrophilic metabolites, which can then be pumped out of the body [2-5].

Xenobiotic transporters have broad substrate specificity, and are involved in both uptake (influx) and secretion (efflux), thereby affecting cellular disposition of their substrates [6]. Therefore, it would be reasonable that both metabolic enzymes and transporters are expressed in skin to act cooperatively as barrier systems against environmental stress and toxins. Indeed, several transporter genes are expressed in both mouse and human skin [2, 7, 8].

Interplay between a metabolic enzyme, cytochrome P450 3A, and an ATP binding cassette (ABC) transporter, P-glycoprotein (P-gp/ABCB1), has been suggested to occur in the metabolism and secretion of xenobiotics in a certain organ [9]. ABC transporters are one of the major xenobiotic transporter superfamilies and use ATP hydrolytic energy as a driving force for efflux pumping of various types of compounds [10]. Although such an interplay has not been demonstrated in skin, the functional expression of one of the ABC transporters, multidrug

resistance-associated protein 1 (MRP1/ABCC1), in mouse skin was recently demonstrated by using *mrp1* gene knockout mice, which exhibited an increase in the accumulation of two MRP1 substrates, fluo 3 (1-[2-amino-5-(2,7-dichloro-6-hydroxy-3-oxo-9-xanthenyl)phenoxy]-2-(2-amino-5-methylphenoxy)ethane-N, N, N, N-tetraacetic acid) and grepafloxacin, in the skin compared with wild-type mice, suggesting that Mrp1 is involved in efflux of these compounds from the skin [11]. Organic anion transport system(s) have also been proposed to be involved in transdermal absorption of flurbiprofen, a nonsteroidal anti-inflammatory drug (NSAID) which exhibits higher transdermal permeability than other NSAIDs [12].

P-gp is another well-characterized ABC transporter which accepts various types of compounds as substrates [13]. It is a product of multidrug resistance (*MDR1*) gene in humans, whereas two subtype genes, *mdr1a* and *mdr1b*, are present in mice [13]. P-gp functions as an efflux pump for various drugs in tissues such as brain, intestine and kidney [13]. In particular, the distribution to the brain of various drugs is greatly limited by the function of P-gp expressed in brain capillary endothelial cells [14, 15]. Despite the accumulated information on the fundamental role of P-gp in drug disposition, the function and expression of P-gp in the skin have not yet been fully characterized. We have already detected gene expression of *MDR1* in human skin, and *mdr1a* and *mdr1b* in mouse skin [8]. P-gp was also detected immunohistochemically in human skin and neonatal mouse skin [2, 16]. The cooperative increase in the expression of P-gp and P450 3A in skin in response to dexamethasone treatment may imply an interplay between P-gp and metabolic enzymes in skin [2]. However, there is no report about the role of P-gp in drug disposition in the

skin. Considering the clinical importance of transdermal therapeutic systems, it seems important to investigate the transport mechanism underlying transdermal drug permeation.

The purpose of the present study was to clarify the role of P-gp in drug disposition in skin, focusing on transdermal drug permeation from the epidermal side and on drug distribution from circulating blood to the skin by using P-gp gene knockout (*mdr1a/1b*$^{-/-}$) mice. To investigate the role of P-gp, the transdermal permeation of P-gp substrates was first examined by means of an Ussing-type chamber method in both absorptive and secretory directions. To further investigate the contribution of P-gp *in vivo*, P-gp substrates were transdermally or intravenously administered, and the concentrations in skin and plasma were analyzed. To more clearly observe the function of P-gp in the skin, we performed the Ussing-type chamber experiment and *in vivo* transdermal administration with tape-stripped mouse skin from which the stratum corneum had been removed, because transporters would function in viable skin layer (viable epidermis and dermis), but not in stratum corneum that consists of dead cells. In addition, we reported that the Ussing-type chamber method with tape-stripped skin may be useful to investigate the role of carrier-mediated transport systems in transdermal drug permeation [12].

Materials and methods

2.1. Materials

Rhodamine 123 (2-[6-amino-3-imino-3H-xanthen-9-yl]benzoic acid methyl ester) and FITC-dextran (fluorescein isothiocyanate-dextran) were purchased from Sigma Chemical Co. Ltd. (St. Louis, MO), itraconazole from LKT Laboratories Inc. (St. Paul, MN), and clotrimazole from Wako Pure Chemical Industries Ltd. (Osaka, Japan). All other reagents were commercial products of reagent grade, and were used without further purification.

2.2. Animals

Six- to nine-week-old male FVB/mdr1a/1b$^{-/-}$ and FVB/ mdr1a/1b$^{+/+}$ mice were purchased from Taconic (Germantown, NY, USA) and CLEA Japan Inc. (Tokyo, Japan), respectively. The mice were kept in a temperature- and light-controlled environment with standard food and tap water provided ad libitum. Animal experiments were performed in accordance with the Guidelines for the Care and Use of Laboratory Animals in Kanazawa University. Three days before experiments, mouse was anesthetized with 1.3 μL/g body weight of sodium pentobarbital (64.8 mg/mL) subcutaneously administered, and the fur over the abdominal skin was removed using an electric hair clipper and depilatory cream.

2.3. Transdermal permeation assessed with an Ussing-type chamber

The permeation experiments were performed by means of an Ussing-type chamber method with tape-stripped mouse skin [12]. Briefly, a mouse was sacrificed under ether anesthesia, and the abdominal skin was stripped using vinyl tape (Nichiban Co., Tokyo, Japan) until the surface glittered (8 times). The skin was excised and mounted vertically in an Ussing-type chamber that provided an exposed area of 0.766 cm^2. Hanks' balanced salt solution (HBSS, 136.7 mM NaCl, 5.36 mM KCl, 0.952 mM $CaCl_2 \cdot 2H_2O$, 0.812 mM $MgSO_4 \cdot 7H_2O$, 0.441 mM KH_2PO_4, 0.385 mM Na_2HPO_4, 25 mM D-glucose and 10 mM HEPES, pH 7.4) was applied to both sides of the chamber. The volume of the bathing solution on both sides was 1.2 mL, and the solutions were kept at 37°C and gassed with 95% O_2 / 5% CO_2 to maintain tissue viability during experiments.

To measure the transdermal permeation, rhodamine 123 or FITC-dextran was applied to the hypodermal or epidermal side, and 0.3 mL of solution was withdrawn from the opposite side and replaced with an equal volume of fresh solution at the designated times. The fluorescence of samples was measured using fluorescence plate reader (Tecan Spectrafluor Plus, Tecan Austria, Salzburg, Austria). To compare the permeability through the skin between the two different compounds that were applied at different doses into the donor side, the transdermal permeability was represented as the distribution volume that was calculated by dividing the amount of drug permeated by the concentration of drug applied to the donor side. Namely, the permeated amount per unit area (pmol/cm^2) was divided by the concentration in the applied solution (μM) and shown as distribution volume per unit area (μL/cm^2).

2.4. Transdermal permeation experiments *in vivo*

Rhodamine 123 and FITC-dextran were dissolved in saline (0.4 and 5 mg/mL, respectively) and itraconazole was dissolved in dimethyl sulfoxide (DMSO, 0.5 mg/mL). The solution was applied to a patch for transdermal administration (16 mm diameter, Torii Pharmaceutical Co. Ltd., Tokyo, Japan). A mouse was anesthetized with sodium pentobarbital, the abdominal skin was stripped, and the patch was applied to the stripped region. At 6 h after dosing of rhodamine 123 and FITC-dextran, mice were sacrificed under ether anesthesia, and the abdominal skin and the blood were collected. Skin and blood were also collected at 18 h after dosing of itraconazole. To compare the absolute values in skin distribution between two compounds at different doses, tissue distribution was represented as distribution volume. Namely, the distributed amount of drug per skin weight (ng/mg skin) was divided by the drug concentration in the solution (mg/mL) applied in transdermal administration or that in circulating plasma (μg/mL) after intravenous administration, and shown as distribution volume per skin weight (nL or μL/mg skin).

2.5. Distribution of itraconazole to the skin after intravenous administration

Intravenous administration of itraconazole was performed according to the method of Hostetler *et al*. and Miyama *et al*. with minor modifications [17, 18]. A 10 mg/mL solution of itraconazole was prepared by dissolving the drug in 3-hydroxypropyl cyclodextrin solution. Briefly, 50 μL of propylene glycol and 7.5 μL of 5 M HCl were mixed and heated to 40 ~ 50 °C, then 20 mg of itraconazole was dissolved in the mixture, and the solution was cooled to 20 ~ 30 °C.

3-Hydroxypropyl cyclodextrin was dissolved at the concentration of 400 mg/mL in purified water, and the solution was then added to the itraconazole solution to give a final volume of 2 mL. The solution was adjusted to pH 5.0 with 10 M NaOH.

A mouse was anesthetized with sodium pentobarbital as described above, and itraconazole was injected into the jugular vein at a dose of 5 mg/kg body weight. Blood samples were collected at 5, 20, 40 and 60 min. At 60 min, the skin, the lungs and the brain were excised.

2.6. Measurement of rhodamine, itraconazole and FD-4

Rhodamine 123 concentration in skin and plasma was measured by means of high-performance liquid chromatography (HPLC) according to the method of Ando *et al*. with some modifications [19]. Briefly, a skin sample was homogenized in 1 mL of purified water. The homogenised sample or plasma sample (100 μL) was mixed with 300 μL of methanol and vortexed for 10 min. After centrifugation, 200 μl of the supernatant was centrifuged again. The supernatant was injected into the HPLC system, which consisted of a constant-flow pump (JASCO PU-2080 Plus), a fluorescence detector (JASCO FP-2020 Plus), an automatic sample injector (JASCO AS-2057 Plus) (JASCO International Co., Ltd., Tokyo, Japan), and an integrator (Chromatopac C-R7A, Shimadzu Corporation, Kyoto, Japan). The fluorescence detector was set at an excitation wavelength of 485 nm and emission wavelength of 565 nm. A reversed-phase column, TSKgel ODS-80TS (4.6 mm x 150 mm; Tosoh, Tokyo, Japan), was maintained at 40 °C in a column oven

(JASCO CO-2065 Plus; JASCO International Co., Ltd.). The mobile phase consisted of 1% acetic acid (pH 4.0) and acetonitrile (7:3, v/v). The flow rate was 1.0 mL/min.

Itraconazole concentration in plasma and tissues was measured by HPLC as reported [20-22], with some modifications. A plasma sample was spiked with the internal standard, clotrimazole, and buffered at pH 7.8 with 0.05 M KH_2PO_4. After vortex-mixing, extraction was performed twice with 4 mL of heptane-isoamyl alcohol (98.5 : 1.5, v/v). The organic phase was back-extracted with 3 mL of 0.05 M H_2SO_4 and removed. The remaining acidic phase was alkalinized to pH 9 with 25% ammnonia solution, and extraction was performed twice with 4 mL of heptane-isoamyl alcohol mixture again. The organic phase was evaporated to dryness under a stream of nitrogen at 55 ˚C. The residue was dissolved in the mobile phase and injected into the HPLC. A skin sample was homogenized in 0.5 mL of purified water and spiked with the internal standard. Then 0.5 mL of 5 N NaOH was added to the homogenized sample, and the sample was solubilized for 15 min at 75 ˚C. Next, 1 mL of 5 M ammonium acetate was added to the lysate, and the sample was extracted in the same way as described for plasma. Lung and brain samples were homogenized in 0.36 and 0.6 mL of purified water, respectively, and each homogenized sample was extracted as described in the case of plasma. The UV detector (JASCO UV-2075 Plus) was set at 263 nm. A reversed-phase column, COSMOSIL 5C18-MS-II (4.6 x 150 mm; Nacalai Tesque, Inc.), was used with a mobile phase of 0.05 % diethylamine in water and acetonitrile (40 : 60, v/v). The flow rate was 1.0 mL/min. Tissue-to-plasma concentration ratio of itraconazole was calculated by dividing the tissue concentration by the plasma concentration.

To measure FD-4 concentration, a skin sample was homogenized in 0.5 mL of purified water. Then 0.5 mL of 5 N NaOH was added to the homogenized sample, and the sample was solubilized for 15 min at 75˚C. Next, 1 mL of 5 M ammonium acetate and 2 mL of heptane-isoamyl alcohol (98.5 : 1.5, v / v) were added to the lysate. The mixture was shaken for 30 min, and centrifuged at 1000 g for 10 min. The organic phase was removed, and 2 mL of heptane-isoamyl alcohol mixture was added to the water layer. After shaking and centrifugation, the organic phase was removed, and the fluorescence of the water phase was measured using a fluorescence plate reader.

2.7. Immunocytochemical analysis

Immunostaining of P-gp in mouse skin was performed according to the method of Sleeman *et al*. and Kato *et al.* with some modifications [16, 23]. The abdominal skin was embedded in optimal cutting temperature (OCT) compound, then quickly frozen in liquid nitrogen and stored at -80 °C until use. The frozen tissue was sectioned with a cryostat, and tissue sections were mounted on glass slides. Before staining, skin sections were fixed in ice-cold acetone for 30 sec and incubated in the mixture of 1% BSA and 5% skim milk for 30 min. Samples were then incubated with the monoclonal antibody against P-gp (C219) for 1 hr at room temperature, and subsequently with Alexa Fluor 488 goat anti-mouse IgG for 30 min. Finally, they were mounted in VECTASHIELD mounting medium with DAPI (Vector Laboratories, Burlingame, CA) to fix the sample and stain the nuclei.

2.8. Statistical analysis

All experiments were performed at least three times. Data are expressed as mean ± S.E.M. Student's t-test was used to determine the statistical significance of differences between two groups. One-way analysis of variance (ANOVA) followed by Dunnett's test was used to determine the statistical significance in comparisons of more than two groups. A p value of less than 0.05 was considered as statistically significant.

Results

3.1. Transdermal permeation of rhodamine 123 assessed in an Ussing-type chamber

Fig. 1 shows the transdermal permeation of a P-gp substrate, rhodamine 123, and a marker compound which permeates through the aqueous domain, FD-4, examined by means of Ussing-type chamber method. The absorptive permeation (from the epidermal to hypodermal side) of rhodamine 123 in *mdr1a/1b*$^{-/-}$ mice was significantly lower than that in wild-type mice (Fig. 1A). On the other hand, the secretory permeation (from the hypodermal to epidermal side) of rhodamine 123 in *mdr1a/1b*$^{-/-}$ mice was significantly higher than that in wild-type mice (Fig. 1B). Rhodamine 123 permeation in wild-type mice thus occurred preferentially in the absorptive direction, whereas that in *mdr1a/1b*$^{-/-}$ mice did not (Fig. 1A, 1B). The transdermal permeation of FD-4 was similar in wild-type and *mdr1a/1b*$^{-/-}$ mice in both directions (Fig. 1C, 1D). The rhodamine 123 permeation in both strains were higher than that of FD-4, indicating that the transcellular pathway might be the major route for the transdermal permeation of rhodamine 123.

3.2. Transdermal permeation of rhodamine 123 and itraconazole *in vivo*

To further examine the permeation of P-gp substrates in the absorptive direction *in vivo*, a patch for transdermal administration was employed. Fig. 2 shows the distribution of rhodamine 123 and FD-4 to the skin after transdermal administration. The distribution of rhodamine 123 in *mdr1a/1b*$^{-/-}$ mice was significantly lower than that in wild-type mice (Fig. 2A). On the other hand, the distribution of FD-4 was similar in wild-type and *mdr1a/1b*$^{-/-}$ mice (Fig. 2B), and lower than

that of rhodamine 123, indicating that the difference in skin distribution of rhodamine 123 between the two strains cannot be explained simply by a difference in the distribution to extracellular space. Plasma concentration of rhodamine 123 was below the detection limit at all the sampling points (< 10 ng/mL of plasma) probably because of small amount applied (~ 40 μg) to the patch due to the dissolution limit of rhodamine 123 in saline.

To further support the involvement of P-gp, the distribution of itraconazole was examined *in vivo*. Itraconazole is applied for the treatment of fungal infections of the skin and is known to be a P-gp substrate [18, 24, 25]. Fig. 3 shows that the distribution of itraconazole to the skin after transdermal administration was significantly lower in *mdr1a/1b*$^{-/-}$ mice than that in wild-type mice. The effect of P-gp inhibitors on the distribution of itraconazole to the skin was then examined. In a preliminary study, the effect of the P-gp substrates or inhibitors verapamil, propranolol and celiprolol [25-27] was examined in wild-type mice. Coadministration of each of them decreased the distribution of itraconazole to the skin, but propranolol had the greatest effect (data not shown). In addition, propranolol is the potential candidate for the transdermal drug delivery [28], since oral bioavailability of propranolol is quite low due to significant first-pass hepatic metabolism [29], but propranolol may be permeable through the skin at least to some extent [28]. Therefore, the effect of propranolol was further examined in both wild-type and *mdr1a/1b*$^{-/-}$ mice. The distribution of itraconazole was decreased by the coadministration of propranolol in wild-type mice, but not in *mdr1a/1b*$^{-/-}$ mice (Fig. 3). In our preliminary study, more typical P-gp inhibitor like varapamil than propranolol had weaker effects on the distribution of itraconazole to the skin. Although the reason

for this finding is unknown, permeability of inhibitors themselves through the skin may also have to be considered to discuss potential inhibition of P-gp functionally expressed in the skin, because not only the affinity of inhibitors for P-gp, but also the concentration of inhibitors available in the skin would affect the inhibition potential for P-gp expressed in the skin. Plasma concentration of itraconazole was below the limit of detection (< 0.5 μg/mL of plasma).

3.3. Distribution of itraconazole from circulating blood to the skin

To examine the skin distribution from the blood side, itraconazole was intravenously administered, and both plasma concentration and skin distribution were determined (Fig. 4). The plasma concentration of itraconazole was similar in wild-type and *mdr1a/1b*$^{-/-}$ mice (Fig. 4A), whereas the tissue-to-plasma concentration ratio at 60 min after administration in the skin of *mdr1a/1b*$^{-/-}$ mice was significantly higher than that in wild-type mice (*mdr1a/1b*$^{-/-}$/wild-type ratio = 1.4). The tissue-to-plasma concentration ratio in the brain of *mdr1a/1b*$^{-/-}$ was also significantly higher than that in wild-type mice, whereas that in the lung of *mdr1a/1b*$^{-/-}$ tended to be higher, but not significantly so, than that in wild-type mice. Such differences in the contribution of P-gp between brain and lung were in good agreement with reported data [18].

3.4. Localization of P-gp in mouse skin

Although we have already demonstrated gene expression of *mdr1a* and *mdr1b* in mouse skin [8], information on the localization of their gene products is limited. Fig. 5 shows the result of immunohistochemical analysis of P-gp in mouse skin. P-gp was observed throughout the dermal and hypodermal (subcutaneous) layers of wild-type mice, while fluorescence staining was absent in those layers of *mdr1a/1b*$^{-/-}$ mice (Fig. 5). Fluorescence observed in the cornified layer could be nonspecific since it was observed not only in wild-type mice, but also in *mdr1a/1b*$^{-/-}$ mice (Fig. 5). It was previously reported that immunoreactive staining against P-gp antibody was detected in the epidermis and the eccrine part of the sweat glands [2, 16, 30]. In the present study, on the other hand, the expression of P-gp was mainly detected in the dermis, but unclear in the epidermis or the eccrine part of the sweat glands. It is generally considered that substances tend to enter the bloodstream via the capillary bed near to the epidermal-dermal junction after transdermal administration. Therefore, if P-gp is only expressed in dermis and/or hypodermis, P-gp may not play fundamental role in transdermal absorption of its substrate to the bloodstream. However, the present finding alone cannot rule out the possibility of the expression of relatively lower amount of P-gp in epidermis, since the detection of P-gp in epidermis may be hindered due to the much higher P-gp expression in dermis and hypodermis regions. Further studies are necessary to clarify physiological role of P-gp expressed in each region of the skin.

Discussion

P-gp has been shown to be involved in drug distribution and excretion in various organs, including intestine, liver and kidney [13]. Nevertheless, the contribution of P-gp to transdermal drug permeation has remained unknown. In the present study, we demonstrate that P-gp contributes to the *in vivo* transport of substrates in the absorptive direction in skin (Figs. 2, 3). Specifically, after transdermal administration, the distribution of rhodamine 123 and itraconazole to the skin in *mdr1a/1b*$^{-/-}$ mice was lower than that in wild-type mice (Figs. 2A, 3), whereas that of FD-4 was similar in the two strains (Fig. 2B). Further, the coadministration of propranolol (a P-gp inhibitor) decreased the itraconazole distribution in skin in wild-type mice, but not in *mdr1a/1b*$^{-/-}$ mice (Fig. 3). These results suggest that P-gp contributes to itraconazole absorption into the skin after transdermal administration. This finding was unexpected, since P-gp is generally considered to play a role as a barrier system to pump out xenobiotic compounds from the body. However, the occurrence of P-gp-mediated absorption was also supported by Ussing-type chamber studies: the transdermal permeation of rhodamine 123 in wild-type mice was shown to be vectorial, favoring the absorptive direction, whereas that in *mdr1a/1b*$^{-/-}$ mice was not (Fig. 1A, 1B). No vectorial permeation of an extracellular marker, FD-4, was observed in either of the strains (Fig. 1, C, D). In the transdermal administration of itraconazole, DMSO was used as a vehicle according to the previous reports [31, 32]. On the other hand, DMSO was reported to extract lipids and interact with keratin in the skin [33]. Therefore, the skin damage cannot be excluded during the transdermal administration of itraconazole for 18 h in the present study. However, there was no obvious morphological difference

in the skin at the end of transdermal administration between itraconazole and rhodamine 123 (administered for 6 h using saline as a vehicle). In addition, the difference in distribution of itraconazole to the skin was observed between wild-type and *mdr1a/1b*$^{-/-}$ mice (Fig. 3). Therefore, the present finding may suggest possible involvement of P-gp in distribution of itraconazole to the skin, although further studies using other P-gp substrates and solvents are necessary to confirm this hypothesis.

On the other hand, when itraconazole was intravenously administered, the tissue-to-plasma concentration ratio in the skin was significantly higher in *mdr1a/1b*$^{-/-}$ mice than that in wild-type mice, as in the case of brain (Fig. 4, B). In brain, P-gp is expressed on luminal membranes of capillary endothelial cells and exports its substrates into the blood [14, 15]. Similarly, the present findings can be explained if we consider that P-gp is involved in the efflux of its substrates from skin to blood. Verapamil, a P-gp substrate, inhibited the efflux of rhodamine 123 in fibroblasts isolated from human dermis [34], also supporting the existence of P-gp-mediated efflux. Although the physiological role of P-gp-mediated efflux from skin to the blood is unknown, it should be noted that skin has a large organ volume (more than twice that of the liver), of which 30% represents interstitial fluid that contains albumin at a similar level to that in plasma [35, 36]. Skin may therefore act as a storage depot for hydrophobic xenobiotics. In addition, various types of metabolic enzymes that also recognize xenobiotic compounds are expressed in skin [2-5]. Therefore, the skin may play a role in capturing the xenobiotic compounds present in the circulating blood, and converting them into hydrophilic metabolites. In the skin, not only P-gp, but also other ABC

transporters, MRP1 and BCRP, are functionally expressed [2, 8, 11, 37]. Therefore, these efflux transporters may contribute to the export of such metabolites into circulating blood. In addition, the passive influx and subsequent P-gp-mediated efflux might enhance the efficiency of metabolism, because the blood flow rate per organ volume in the skin is much smaller than in other organs [35, 36], so the interplay of enzyme-transporter interactions may be similar to that in the small intestine [9].

Fluconazole is another triazole antifungal agent that is employed to treat skin infection [38]. A study in guinea pigs indicated that the distribution of itraconazole to the epidermis and hypodermis after systemic administration was much lower than that of fluconazole, even though the plasma concentrations of these drugs are similar [38]. This observation was previously explained in terms of differences in binding to keratin between itraconazole and fluconazole [38]. However, the affinity of itraconazole for P-gp (IC_{50} < 3 μM) is much higher than that of fluconazole (IC_{50} > 400μM) [25, 39]. Therefore, our present finding regarding the contribution of P-gp to the transport of itraconazole from skin to blood may indicate that P-gp expressed in the skin effectively transports itraconazole from skin to blood, resulting in a lower distribution to the skin, compared with that of fluconazole.

Involvement of P-gp in drug absorption in the skin could have significant implications for drug development, given that P-gp has a broad substrate specificity [13]. Oral administration of P-gp substrates can be problematic, since intestinal P-gp limits their absorption from the intestinal tract [6]. In skin, on the other hand, P-gp may serve to increase distribution from the epidermal side

to the skin (Figs. 2, 3). This finding may have impact on the selection of a suitable administration route for P-gp substrates. In addition, several single-nucleotide polymorphisms in *MDR1* gene are known to alter the expression and/or function of P-gp [13]. This may cause interindividual differences in the kinetics of drug disposition in the skin. For example, sparfloxacin and levofloxacin, both of which are fluoroquinolones and P-gp substrates, cause adverse dermatological reactions, such as photosensitivity dermatitis [40, 41]. Further analysis should be performed to clarify the possible relevance of P-gp to such adverse reactions. In the present study, however, plasma concentrations of rhodamine123 and itraconazole after transdermal administration were below the limit of detection, probably because of limited permeation of these compounds through the skin. In addition, the present analysis has not yet analyzed details in substrate specificity of P-gp functionally expressed in the skin. Only limited numbers of substrate and inhibitor of P-gp were used in the present study because of the limited permeability of commercially available P-gp substrates through the skin. Therefore, the present finding is the first step to clarify the involvement of P-gp in dermal drug disposition. Investigations using more permeable drugs will also be necessary to demonstrate important implications of P-gp for the delivery of therapeutic agents into and through the skin.

It should be noted that the phenotype regarding skin distribution in *mdr1a/1b*$^{-/-}$ mice was different between transdermal and intravenous administrations. The distribution to the skin was decreased by *mdr1a/1b*$^{-/-}$ knockout after transdermal administration (Fig. 2, 3), whereas it was increased after intravenous injection (Fig. 4). Possible explanations include uneven localization of

P-gp, leading to a difference in the contributions of P-gp to permeability from the epidermal side into the skin and from skin to blood. In the present study, immunohistochemical analysis revealed that P-gp is expressed in dermis, although the polarity of P-gp expression in the dermal cells was not clearly observed (Fig. 5). The skin consists of multilayers of various differentiated and undifferentiated cells, and therefore the distribution of localization and/or function of transporters also needs to be clarified.

In the present study, stratum corneum had been removed by tape-stripping despite the poor permeability barrier of mouse skin compared to human skin. In clinical applications, skin is rarely tape-stripped prior to application of a transdermal patch. Furthermore, it is believed that stratum corneum is the rate-determining step for the transdermal permeation of most drug molecules. Therefore, further study with intact skin is needed to investigate the clinical relevance of the P-gp function in the skin. In addition, to avoid possible saturation of P-gp, we attempted to use the lowest concentration of rhodamine 123 in Usssing-type chamber by considering the detection limit. Therefore, the substrate concentration in the present study may be much lower than that typically applied in transdermal systems. Since the contribution of P-gp in dermal drug disposition may depend on the substrate concentration, investigations using P-gp substrates at clinically relevant concentration range are also needed to clarify clinical implication of P-gp in transdermal drug delivery.

In conclusion, our present findings indicate that P-gp contributes to the transport of its substrates both from the epidermal side into the skin, and from skin to blood. Because many drugs

are reported to be substrates for P-gp [13], it is also implied that P-gp contributes to the dermal disposition of other P-gp substrates than rhodamine 123 and itraconazole. Therefore, further studies in intact skin with stratum corneum are needed to clarify clinical implications of P-gp for the delivery of therapeutic agents into and through the skin.

Acknowledgement

We thank Ms Lica Ishida for technical assistance with LC-MS/MS. We also thank Ms Emi Nambu for performing animal experiments. This study was supported in part by a Grant-in-Aid for Scientific Research provided by the Ministry of Education, Science and Culture of Japan.

References

[1] C.R. Harding, The stratum corneum: structure and function in health and disease, Dermatol. Ther. 17(Suppl 1) (2004) 6-15.

[2] J.M. Baron, D. Holler, R. Schiffer, S. Frankenberg, M. Neis, H.F. Merk, F.K. Jugert, Expression of multiple cytochrome p450 enzymes and multidrug resistance-associated transport proteins in human skin keratinocytes, J. Invest. Dermatol. 116(4) (2001) 541-548.

[3] F.K. Jugert, R. Agarwal, A. Kuhn, D.R. Bickers, H.F. Merk, H. Mukhtar, Multiple cytochrome P450 isozymes in murine skin: induction of P450 1A, 2B, 2E, and 3A by dexamethasone, J. Invest. Dermatol. 102(6) (1994) 970-975.

[4] D.S. Keeney, C. Skinner, S. Wei, T. Friedberg, M.R. Waterman, A keratinocyte-specific epoxygenase, CYP2B12, metabolizes arachidonic acid with unusual selectivity, producing a single major epoxyeicosatrienoic acid, J. Biol. Chem. 273(15) (1998) 9279-9284.

[5] D.S. Keeney, C. Skinner, J.B. Travers, J.H. Capdevila, L.B. Nanney, L.E. King Jr, M.R. Waterman, Differentiating keratinocytes express a novel cytochrome P450 enzyme, CYP2B19, having arachidonate monooxygenase activity, 273(48) (1998) 32071-32079.

[6] A. Tsuji, Transporter-mediated Drug Interactions, Drug Metab. Pharmacokinet. 17(4) (2002) 253-274.

[7] R. Schiffer, M. Neis, D. Holler, F. Rodriguez, A. Geier, C. Gartung, F. Lammert, A. Dreuw, G. Zwadlo-Klarwasser, H. Merk, F. Jugert, J.M. Baron, Active influx transport is mediated by

members of the organic anion transporting polypeptide family in human epidermal keratinocytes, J. Invest. Dermatol. 120(2) (2003) 285-291.

[8] Q. Li, H. Tsuji, Y. Kato, Y. Sai, Y. Kubo, A. Tsuji, Characterization of the transdermal transport of flurbiprofen and indomethacin, J. Control. Release. 110(3) (2006) 542-556.

[9] L.Z. Benet, C.L. Cummins, C.Y. Wu, Unmasking the dynamic interplay between efflux transporters and metabolic enzymes, Int. J. Pharm. 277(1-2) (2004) 3-9.

[10] P. Borst, R.O. Elferink, Mammalian ABC transporters in health and disease, Annu. Rev. Biochem. (2002) 71 537-592.

[11] Q. Li, Y. Kato, Y. Sai, T. Imai, A. Tsuji, Multidrug resistance-associated protein 1 functions as an efflux pump of xenobiotics in the skin, Pharm. Res. 22 (6) (2005) 842–846.

[12] K. Ito, Y. Kato, H. Tsuji, T. N. Hai, Y. Kubo, A. Tsuji, Involvement of organic anion transport system in transdermal absorption of flurbiprofen. J. Control. Release. 124(1-2) (2007) 60-68.

[13] C. Marzolini, E. Paus, T. Buclin, R.B. Kim, Polymorphisms in human MDR1 (P-glycoprotein): recent advances and clinical relevance. Clin. Pharmacol. Ther., 75(1) (2004) 13-33.

[14] A. Tsuji, T. Terasaki, Y. Takabatake, Y. Tenda, I. Tamai, T. Yamashima, S. Moritani, T. Tsuruo, J. Yamashita, P-glycoprotein as the drug efflux pump in primary cultured bovine brain capillary endothelial cells. Life Sci. 51(18) (1992) 1427-1437.

[15] A.H. Schinkel, J.J. Smit, O. van Tellingen, J.H. Beijnen, E. Wagenaar, L. van Deemter, C.A. Mol, M.A. van der Valk, E.C. Robanus-Maandag, H.P. te Riele, Disruption of the mouse mdr1a

P-glycoprotein gene leads to a deficiency in the blood-brain barrier and to increased sensitivity to drugs. Cell. 77(4) (1994) 491-502.

[16] M.A. Sleeman, J.D. Watson, J.G. Murison, Neonatal murine epidermal cells express a functional multidrug-resistant pump, J. Invest. Dermatol. 115(1) (2000) 19-23.

[17] J.S. Hostetler, L.H. Hanson, D.A. Stevens, Effect of cyclodextrin on the pharmacology of antifungal oral azoles, Antimicrob. Agents Chemother. 36(2) (1992) 477-480.

[18] T. Miyama, H. Takanaga, H. Matsuo, K. Yamano, K. Yamamoto, T. Iga, M. Naito, T. Tsuruo, H. Ishizuka, Y. Kawahara, Y. Sawada, P-glycoprotein-mediated transport of itraconazole across the blood-brain barrier, Antimicrob. Agents Chemother. 42(7) (1998) 1738-1744.

[19] H. Ando H, Y. Nishio, K. Ito, A. Nakao, L. Wang, Y.L. Zhao, Effect of endotoxin on P-glycoprotein mediated biliary and renal excretion of rhodamine-123 in rats, Antimicrob. Agents Chemother. 45(12) (2001) 3462–3467.

[20] R. Woestenborghs, W. Lorreyne, J. Heykants, Determination of itraconazole in plasma and animal tissues by high-performance liquid chromatography, J. Chromatogr. 413 (1987) 332–337.

[21] S. Sobue, K. Sekiguchi, T. Nabeshima, Intracutaneous distributions of fluconazole, itraconazole, and griseofulvin in Guinea pigs and binding to human stratum corneum, Antimicrob. Agents Chemother. 48(1) (2004) 216-223.

[22] A.K. Gupta, K. Groen, R. Woestenborghs, P. De Doncker, Itraconazole pulse therapy is effective in the treatment of Majocchi's granuloma: a clinical and pharmacokinetic evaluation and implications for possible effectiveness in tinea capitis, Clin. Exp. Dermatol. 23(3) (1998) 103-108.

[23] Y. Kato, M. Sugiura, T. Sugiura, T. Wakayama, Y. Kubo, D. Kobayashi, Y. Sai, I. Tamai, S. Iseki, A. Tsuji, Organic cation/carnitine transporter OCTN2 (Slc22a5) is responsible for carnitine transport across apical membranes of small intestinal epithelial cells in mouse, Mol. Pharmacol. 70(3) (2006) 829-837.

[24] D. Balayssac, N. Authier, A. Cayre, F. Coudore, Does inhibition of P-glycoprotein lead to drug-drug interactions?, Toxicol. Lett. 156(3) (2005) 319-329.

[25] D. Schwab, H. Fischer, A. Tabatabaei, S. Poli, J. Huwyler, Comparison of in vitro P-glycoprotein screening assays: recommendations for their use in drug discovery, J. Med. Chem. 46(9) (2003) 1716-1725.

[26] I. Bachmakov, U. Werner, B. Endress, D. Auge, F.M. Fromm, Characterization of beta-adrenoceptor antagonists as substrates and inhibitors of the drug transporter P-glycoprotein, Fundam. Clin. Pharmacol. (2006) 20(3) 273-282.

[27] T. Terao, E. Hisanaga, Y. Sai, I. Tamai, A. Tsuji, Active secretion of drugs from the small intestinal epithelium in rats by P-glycoprotein functioning as an absorption barrier, J. Pharm. Pharmacol. 48(10) (1996) 1083-1089.

[28] A. Namdeo, N.K. Jain, Liquid crystalline pharmacogel based enhanced transdermal delivery of propranolol hydrochloride, J. Control. Release. 82(2-3) (2003) 223-236.

[29] J.G. Riddell, D.W. Harron, R.G. Shanks, Clinical pharmacokinetics of beta-adrenoceptor antagonists, An update, Clin. Pharmacokinet. 12(5) (1987) 305-320.

[30] A. Bittl, M. Nap, W. Jäger, F. Cornillie, N. Lang, Immunohistochemical detection of P-glycoprotein on frozen and paraffin-embedded tissue sections of normal and malignant tissues, Anticancer Res. 15(3) (1995) 1007-1014.

[31] G.E. Gutierrez, D. Lalka, I.R. Garrett, G. Rossini, G.R. Mundy, Transdermal application of lovastatin to rats causes profound increases in bone formation and plasma concentrations, Osteoporos Int. 17(7) (2006) 1033-1042.

[32] X.S. Zheng, C.Z. Duan, Z.D. Xiao, B.A. Yao, Transdermal delivery of praziquantel: effects of solvents on permeation across rabbit skin, Biol Pharm Bull. 31(5) (2008) 1045-1048.

[33] B.W. Barry, Novel mechanisms and devices to enable successful transdermal drug delivery, Eur. J. Pharm. Sci. 14(2) (2001) 101-114.

[34] G. Lizard, M.C. Chignol, Y. Chardonnet, D. Schmitt, Active cell membrane mechanisms involved in the exclusion of RH 123 allow distinction between normal and tumoral cells, Cell Biol. Toxicol. 10(5-6) (1994) 399-406.

[35] A. Tsuji, T. Yoshikawa, K. Nishide, H. Minami, M. Kimura, E. Nakashima, T. Terasaki, E. Miyamoto, C.H. Nightingale, T. Yamana, Physiologically based pharmacokinetic model for beta-lactam antibiotics I: Tissue distribution and elimination in rats, J. Pharm. Sci. 72(11) (1983) 1239-1252.

[36] A. Tsuji, K. Nishide, H. Minami, E. Nakashima, T. Terasaki, T. Yamana, Physiologically based pharmacokinetic model for cefazolin in rabbits and its preliminary extrapolation to man, Drug Metab. Dispos. 13(6) (1985) 729-739.

[37] C. Triel, M.E. Vestergaard, L. Bolund, T.G. Jensen, U.B. Jensen, Side population cells in human and mouse epidermis lack stem cell characteristics, Exp. Cell Res. 295(1) (2004) 79-90.

[38] S. Sobue, K. Sekiguchi, T. Nabeshima, Intracutaneous distributions of fluconazole, itraconazole, and griseofulvin in Guinea pigs and binding to human stratum corneum, Antimicrob. Agents Chemother. 48(1) (2004) 216-223.

[39] K. Yasuda, L.B. Lan, D. Sanglard, K. Furuya, J.D. Schuetz, E.G. Schuetz, Interaction of cytochrome P450 3A inhibitors with P-glycoprotein. J. Pharmacol. Exp. Ther. 303(1) (2002) 323-332.

[40] Y. Tokura, Quinolone photoallergy: photosensitivity dermatitis induced by systemic administration of photohaptenic drugs, J. Dermatol. Sci. 18(1) (1998) 1-10.

[41] K. Naruhashi, I. Tamai, N. Inoue, H. Muraoka, Y. Sai, N. Suzuki, A. Tsuji, Active intestinal secretion of new quinolone antimicrobials and the partial contribution of P-glycoprotein, J. Pharm. Pharmacol. 53(5) (2001) 699-709.

Figure legends

Fig. 1

Transdermal permeation of rhodamine 123 and FD-4 across tape-stripped skin of wild-type and *mdr1a/1b*$^{-/-}$ mice

Transdermal permeation of rhodamine 123 (0.5 μM) (A, B) and FD-4 (10 μM) (C, D) from the epidermal to the hypodermal side (absorptive direction) (A, C) and from the hypodermal to the epidermal side (secretory direction) (B, D) was measured at 37˚C in Hanks' balanced salt solution. Open and closed symbols represent the transdermal permeation in wild-type and *mdr1a/1b*$^{-/-}$ mice, respectively. The data represent means ± S.E.M. (n = 3 - 9). When error bars are not shown, they were smaller than the symbols.

* Significantly different from wild-type mice ($p < 0.05$).

Fig. 2

Distribution of rhodamine 123 and FD-4 to stripped skin of wild-type and *mdr1a/1b*$^{-/-}$ mice after transdermal administration

Rhodamine 123 (A) and FD-4 (B) distributed to the skin were measured 6 h after the start of transdermal administration. Rhodamine 123 solution (0.4 mg/mL in saline, 100 μL) or FD-4 solution (5 mg/mL in saline, 100 μL) was first applied to a patch for transdermal administration, and then the patch was applied to tape-stripped abdominal skin. Open and grey columns represent

the distribution normalized by the drug concentration in administered solution in wild-type and *mdr1a/1b*$^{-/-}$ mice, respectively. The results are shown as mean ± S.E.M. (n = 3 - 5).

* Significantly different between wild-type and *mdr1a/1b*$^{-/-}$ mice given the same treatment ($p < 0.05$).

Fig. 3

Distribution of itraconazole in stripped skin of wild-type and *mdr1a/1b*$^{-/-}$ mice after transdermal administration

Itraconazole distributed to the skin was measured 18 h after application. Itraconazole solution (0.5 mg/mL DMSO, 50 μL) with or without propranolol (100 mM) was first applied to a patch for transdermal administration, and the patch was applied to tape-stripped abdominal skin. Open and grey columns represent the accumulation in wild-type and *mdr1a/1b*$^{-/-}$ mice, respectively. The amount of distribution was normalized by the drug concentration in administered solution, and results are shown as mean ± S.E.M. (n = 3 - 4).

* Significantly different from wild-type mice without propranolol ($p < 0.05$).

Fig. 4

Distribution of itraconazole in wild-type and *mdr1a/1b*$^{-/-}$ mice after intravenous administration

Itraconazole was intravenously administered at a dose of 5 mg/kg body weight. In panel A, open and grey circles represent the plasma concentration in wild-type and *mdr1a/1b*$^{-/-}$ mice, respectively.

Panel B shows tissue-to-plasma concentration ratio at 60 min after administration in wild-type (open columns) and *mdr1a/1b*$^{-/-}$ mice (grey columns). Data are expressed as mean ± S.E.M (n = 3-4). When error bars are not shown, they were smaller than the symbols.

Fig. 5

Immunohistochemical analysis of P-gp expression in skin from wild-type and *mdr1a/1b*$^{-/-}$ mice

Cryosections (10 μm) of skin from wild (A) and *mdr1a/1b*$^{-/-}$ mice (B) were incubated with anti-P-gp antibody (C219) followed by goat anti-mouse Alexa 488 (green signal). Both sections were counter-stained for nuclei with DAPI (blue signal).

Fig. 1

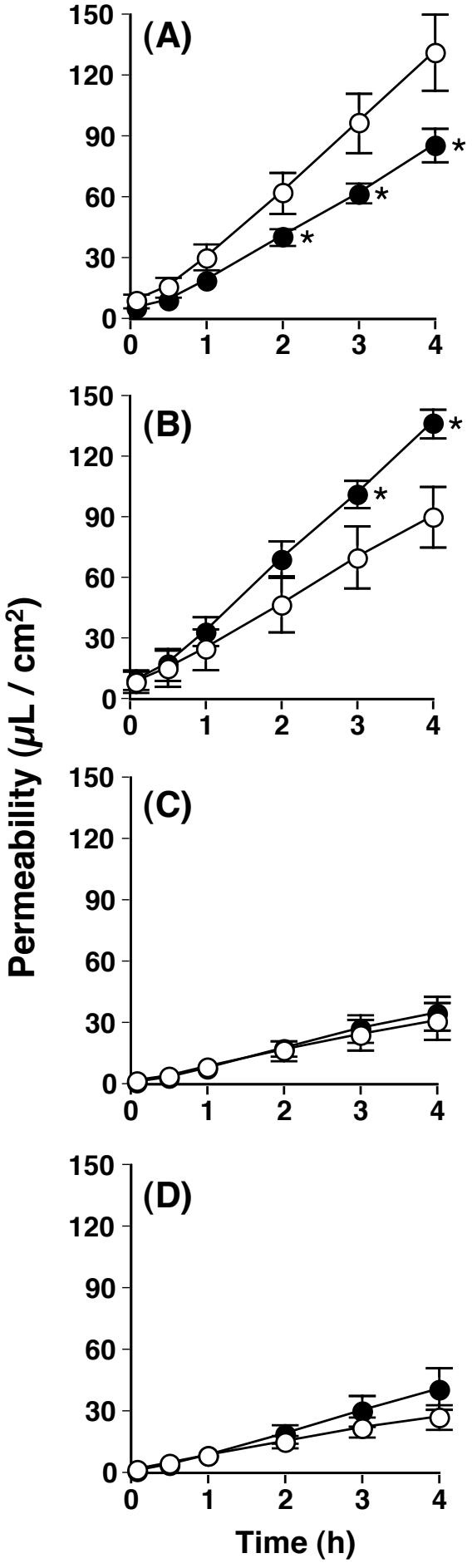

Fig. 2

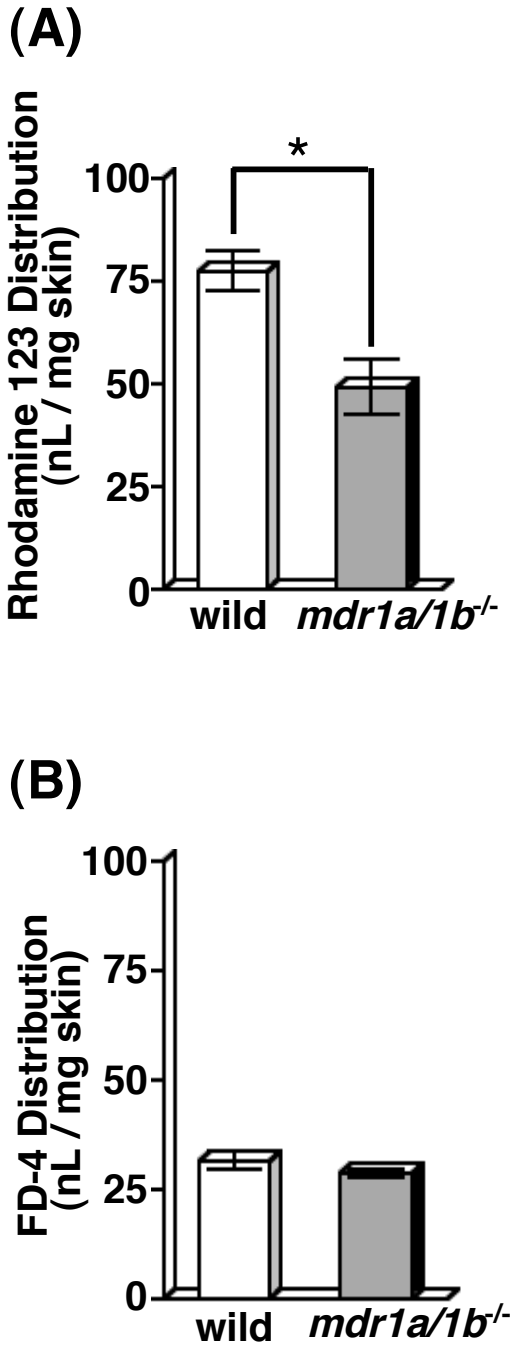
(A)
Rhodamine 123 Distribution
(nL / mg skin)
100
75
50
25
0
*
wild
mdr1a/1b-/-
(B)
FD-4 Distribution
(nL / mg skin)
100
75
50
25
0
wild
mdr1a/1b-/-

Fig. 3

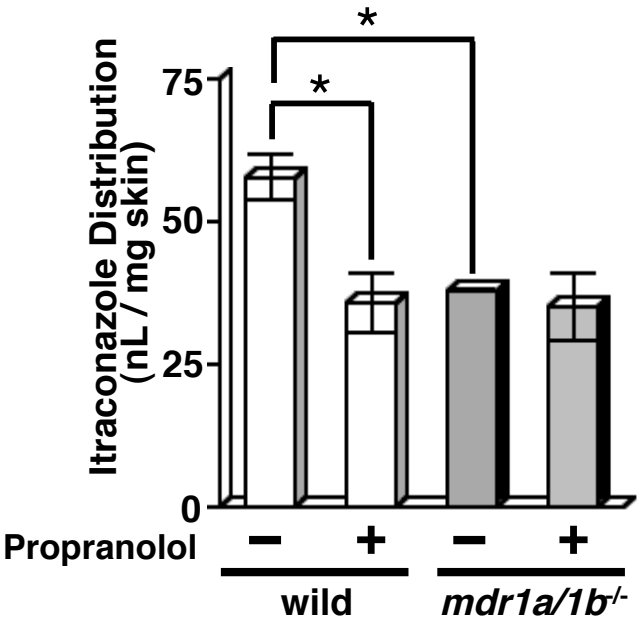
Itraconazole Distribution
(nL / mg skin)
75
50
25
0
*
*
Propranolol
−
+
−
+
wild
mdr1a/1b-/-

Fig. 4

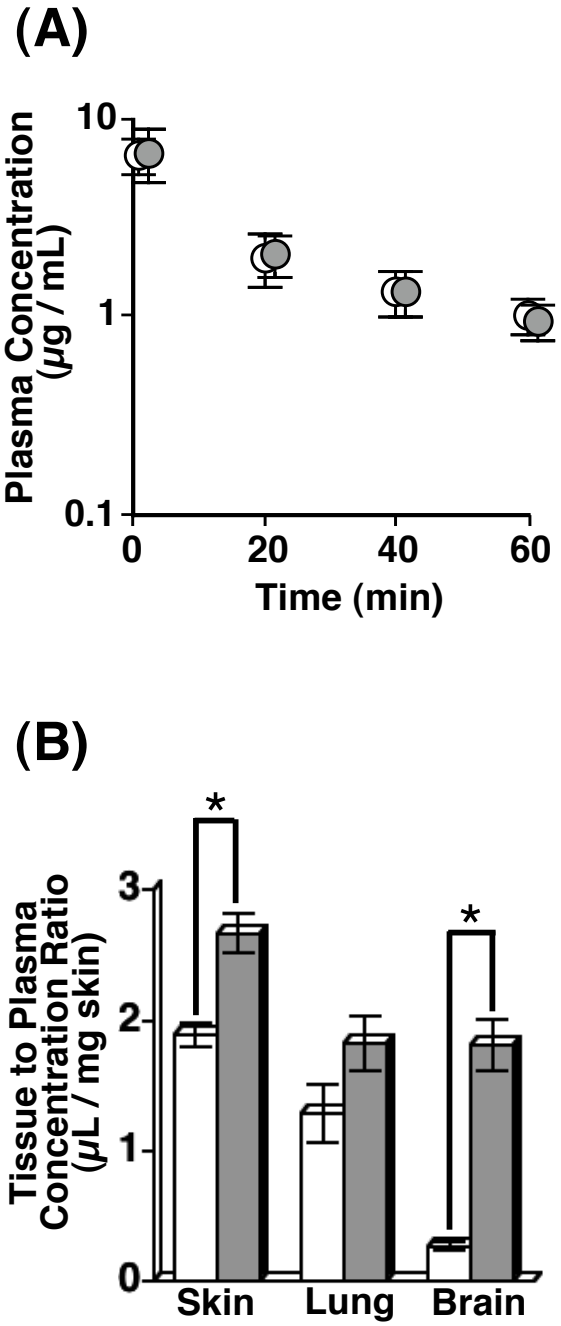
(A)
Plasma Concentration (μg / mL)
10
1
0.1
0
20
40
60
Time (min)
(B)
Tissue to Plasma Concentration Ratio (μL / mg skin)
3
2
1
0
*
*
Skin
Lung
Brain

Fig. 5

(A)

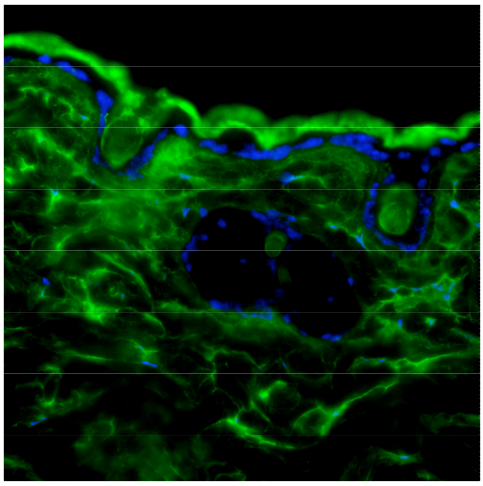

(B)